RSC Advances

PAPER

View Article Online
View Journal | View Issue

Cite this: *RSC Adv.*, 2019, **9**, 29368

Modulation of JNK-1/ β-catenin signaling by *Lactobacillus casei*, inulin and their combination in 1,2-dimethylhydrazine-induced colon cancer in mice†

Mohammed S. Ali,[a] Rasha M. Hussein,[ab]* Yasser Gaber,[bc] Olfat A. Hammam[d] and Mohamed A. Kandeil[e]

Colon cancer is a complex disease that involves numerous genetic alterations that change the normal colonic mucosa into invasive adenocarcinoma. In the current study, the protective effects of inulin (prebiotic), *Lactobacillus casei* (*L. casei*, probiotic) and their combination (synbiotic) on 1,2-dimethylhydrazine (DMH)-induced colon cancer in male Swiss mice were evaluated. Animals were divided into: Control group, DMH-treated group, DMH plus inulin, DMH plus *L. casei* and DMH plus inulin plus *L. casei*-treated groups. Fecal microbiome analysis, biochemical measurements, histopathological examination of the colon tissues, immunostaining and Western blotting analysis of β-catenin, GSK3β and JNK-1 were performed. The prebiotic-, probiotic- and synbiotic-treated groups showed decreased levels of carcinoembryonic antigen and a lower number of aberrant crypt foci compared to the DMH-treated group with the synbiotic group exhibiting a superior effect. Furthermore, all treatments showed a body weight-reducing effect. Administration of inulin, *L. casei* or their combination increased the expression level of phospho-JNK-1 while they decreased the expression level of β-catenin and phospho-GSK3β. Remarkably, *L. casei* treatment resulted in enrichment of certain beneficial bacterial genera *i.e. Akkermansia* and *Turicibacter*. Therefore, administration of *L. casei* and inulin as a synbiotic combination protects against colon cancer in mice.

Received 11th June 2019
Accepted 27th August 2019

DOI: 10.1039/c9ra04388h

rsc.li/rsc-advances

1. Introduction

Colon cancer is the second cause of cancer-related deaths.[1] It is a complex process which involves numerous genetic mutations that eventually change normal colonic mucosa into invasive adenocarcinoma.[1,2] Colon cancer is caused by many predisposing factors such as microbial exposure, imbalanced diet, inflammation, intestinal epithelial damage and, importantly, normal gut microbiota imbalance.[3–5] 1,2-Dimethylhydrazine (DMH) is a chemical compound widely used to induce colon cancer in experimental animals since it shows high pathological similarity with human colon cancer.[6,7]

Probiotics are live microorganisms that have beneficial effects to the host such as immunomodulation and improvement of gut microbiota through improving gut homeostasis and alleviating the inflammation caused by pathogenic strains.[8–11] Interestingly, the administration of probiotics is increasingly used to prevent various human diseases. For example, it was found that administration of a probiotic mixture could prevent the conversion of liver cirrhosis to hepatocellular carcinoma.[12] Also, a mixture of *Bifidobacterium* and *Lactobacillus* species could alleviate chronic kidney failure by reducing the plasma levels of urea, indoxyl sulfate and *p*-cresol.[13] More relevant to this study, probiotics were found to inhibit the development of colon cancers through inducing apoptosis and modulating the cellular defensive mechanisms.[14]

Prebiotics are bioactive substances, fermented by the normal gut microflora to beneficial products such as butyrate and propionate which inhibit colon cancer biomarkers.[15] Inulin is one of the prebiotics which contains a polymer of fructooligosaccharides linked together by β-(2-1) bond and it previously showed an important role in decreasing the pre-cancerous lesions of colon cancer.[16]

[a]*Department of Biochemistry, Faculty of Pharmacy, Beni-Suef University, Salah Salem Street, 62514, Beni-Suef, Egypt. E-mail: rasha.hussein@pharm.bsu.edu.eg; Tel: 002 1200136515*

[b]*Department of Pharmaceutics and Pharmaceutical Technology, College of Pharmacy, Mutah University, 61710, Al-Karak, Jordan*

[c]*Department of Microbiology and Immunology, Faculty of Pharmacy, Beni-Suef University, 62514, Beni-Suef, Egypt*

[d]*Pathology Department, Theodor Bilharz Research Institute, 12411 Giza, Egypt*

[e]*Department of Biochemistry, Faculty of Veterinary Medicine, Beni-Suef University, Egypt*

† Electronic supplementary information (ESI) available. See DOI: 10.1039/c9ra04388h

Interestingly, a combination of probiotic and prebiotic is known as synbiotic and it provides a synergistic effect that improves growth of the beneficial microbiome along with supplying new ones into the colon.[17] Therefore, administration of synbiotics can restore the normal microbiome balance, immunity and consequently reduce the severity of cancer lesions.[18,19]

β-Catenin signaling plays an important role in colon carcinogenesis and its inhibition is viewed as a good target for the action of many chemotherapeutic drugs.[20] More than 90% of the inherited colon cancer cases showed a mutation in the canonical Wnt/β-catenin signaling pathway.[21] Importantly, JNK-1 is a member of Mitogen activated protein kinase (MAPK) family and it negatively regulates the β-catenin expression through its effect on glycogen synthase kinase 3 beta (GSK3β) phosphorylation.[22] Therefore, it was found that some drugs such as sulindac and Pizotifen combat the prostate and colon cancer respectively *via* decreasing β-catenin expression levels.[23,24]

In the current study, we investigated the possible protective effects of inulin (prebiotic), *Lactobacillus casei* (probiotic), and their combination (synbiotic) on DMH-induced colon cancer in male Swiss mice and the role of JNK-1/β-catenin signaling pathway in this process.

2. Materials and methods

2.1. Chemicals

1,2-Dimethylhydrazine dihydrochloride ($C_2H_{10}C_{l2}N_2$) and inulin from chicory were purchased from Acros Organics, Thermo Fisher Scientific, Belgium. *Lactobacillus casei* DSM 20011 (ATCC 393) was purchased from the German collection of microorganisms and cell cultures (DSMZ) Germany. MRS Broth was purchased from the Foreign Trade Association, Egypt.

2.2. Animals

Forty male Swiss mice (6 weeks old, weighing about 25 g) were obtained from Animal House Colony, Pharmacology and Chemistry Research Center, Misr University and Technology Park, Egypt. Mice were kept in plastic cages (8 mice per cage) under the following standard conditions: 12 h light/dark cycles, 25 ± 2 °C temperature, and humidity 48 ± 10% at the Animal House Laboratory at Faculty of Pharmacy, Beni-Suef University. Mice had free access to water and standard pellet diet composed of 14.5% protein, 4.8% fat and 59.4% carbohydrates. All the experimental procedures performed in this study were in agreement with the guidelines of National Institutes of Health guide for use and care of laboratory animals revised in 1978. The study protocol was approved by the Animal Ethics Committee at Beni-Suef University (Approval number: 018-56).

2.3. Bacterial culture and viable counting

Lactobacillus casei DSM 20011 were grown on MRS media adjusted to pH 5.5 and incubated at 30 °C. The grown cells were collected under cooling centrifugation at 1700 × *g* for 15 min. The cells were washed with saline and resuspended in saline to a final a concentration of 2×10^9 CFU/0.3 ml. Optical turbidity was recorded at wavelength 600 nm as a measure of the concentration of bacterial suspension. A calibration curve was constructed between the bacterial optical density and the viable counting to facilitate dose adjustment.

2.4. *In vivo* study

2.4.1. Induction of colon cancer. Mice were injected subcutaneously (SC.) with DMH at a dose of 20 mg kg^{-1} BW dissolved in 1 mM EDTA, pH 6.5 once a week for 20 weeks. Carcinogen dose was selected based on previously published literature to induce colon cancer in mice.[7]

2.4.2. Experimental groups. After two weeks of acclimatization period, mice were divided into 5 groups (8 mice per group) as follows:

Control (untreated) group. Mice received SC. injections of 1 mM EDTA, pH 6.5 once per week for 20 weeks.

DMH-treated group. Mice received SC. injections of DMH as described above.

DMH + inulin (prebiotic) treated group. Mice received SC. injections of DMH as DMH-treated group plus inulin (5 mg/0.3 ml/animal) by oral gavage daily from the start of the experiment till animal sacrifice. The dose of inulin was selected based on the previously published study.[17]

DMH + L. casei (probiotic) treated group. Mice received SC. injections of DMH as DMH-group plus *L. casei* (2×10^9 CFU/0.3 ml per animal) 3 times per week by oral gavage from the start of the experiment till animal sacrifice. The selected bacterial concentration was based on ref. 25.

DMH + inulin + L. casei (synbiotic) treated group. Mice received SC. injections of DMH as DMH-group plus inulin (5 mg/0.3 ml per animal) *via* oral gavage daily plus *L. casei* (2×10^9 CFU/0.3 ml per animal) 3 times per week by oral gavage from the start of the experiment till animal sacrifice.

After 24 weeks, animals were overnight fasting, and blood samples were collected in the morning in heparinized tubes. Plasma was separated by centrifugation at 3000 rpm for 20 min and stored at −80 °C for biochemical measurements. Animals were then anesthetized by diethyl ether and killed by cervical decapitation. The colons were dissected, opened longitudinally, washed with saline and dried on filter paper. A small part of the distal colon was excised and immersed into a protease inhibitor buffer and stored at −80 °C for Western blotting analysis. The remaining part of the colon was kept in 10% buffered formalin solution for histopathology and immunostaining analysis.

2.5. Biochemical measurement in plasma

The concentrations of glucose, triglyceride and total cholesterol were measured in the plasma samples by commercial kits (glucose – TR, triglycerides – LQ and cholesterol assay kits, SPINREACT, Spain respectively) according to the provided instructions.

2.6. Histopathological examination

2.6.1. Macroscopic examination. Colons from all groups were observed macroscopically for the presence of plaque

lesions and if any, their count by an experimentally blinded pathologist.

2.6.2. Microscopic examination. Sections of colons were fixed in 10% formalin buffered solution then embedded in paraffin wax, cut at a 4 μm thickness and stained with Hematoxylin and Eosin (H&E) for microscopic examination under a light microscope as previously mentioned in ref. 26.

2.6.3. Methylene blue staining. To estimate the number of aberrant crypt foci (ACF), the paraffin sections of the formalin fixed colon tissues were used as previously mentioned in ref. 27–30. Briefly, the sections were deparaffinized and hydrated with distilled water. About 1 ml of 0.5% methylene blue solution was applied until the tissue sections were completely covered and incubated for 3 minutes. The slides were briefly rinsed in distilled water (2–3 dips) and left to dry in air. Finally, the slides were cleared in xylene, and mounted in a synthetic resin. The number of ACF was determined in 10 independent fields per animal under a light microscope at 400× magnification.

The number of goblet cells was quantified in the colonic tissues using a computer controlled microscope (Zeiss Axioscope microscope, Germany) and the image analysis was performed using the software program Axio vision 4.8 which allows for the determination of the colored compound in the goblet cells stained with methylene blue. The number of goblet cells was analyzed for each colon/group under a light microscope at 400×.

2.7. Immunohistochemical analysis of the carcinoembryonic antigen (CEA)

Immunostaining of the colon tissues with CEA was performed as follows: the slides were deparaffinized, hydrated, blocked and then stained by CEA monoclonal antibody solution (sc-55547, Santa Cruz Biotechnology, Inc, USA) 1 : 50 dilution for 20 min. The slides were washed followed by applying the secondary antibody; HRP Envision kit, DAKO, Agilent, US (no dilution) for 20 min and applying 3,3′-diaminobenzidine (DAB, Sigma Fast DAB tablets, Sigma-Aldrich, St. Louis MO) for 20 min as previously mentioned.[31] The slides were finally counterstained with EnVision FLEX hematoxylin for 5 min, dehydrated, cleared and covered by a slip. The colonic sections were examined using a Zeiss light microscope (Oberkochen, Germany). The brownish-color was considered as a positive expression of CEA in the cells. Immunostaining expression was classified according to its distribution into either cytoplasmic type, in which immunostaining was homogeneously distributed in the cytoplasm of neoplastic cells or an apical type in which, there was predominant immunostaining on the cytoplasmic edge closest to the lumen of the neoplastic tissue cells.[32] The positively stained cells were recorded within ten successive fields in each sample and quantified using Leica application suite for image analysis at 400× magnification.

2.8. Western blotting analysis

Thirty mg of each colon tissue sample was homogenized in 400 μl ice-cold RIPA buffer. The homogenate was put on a pre-cooled microcentrifuge tube and agitated at 16 000 × *g* for 30 min at 4 °C then spun for 20 min. The supernatant was then collected, and the protein concentration was determined by Bradford assay. 20 μg of protein was mixed with an equal volume of Laemmli buffer and boiled for 5 min at 95 °C to run SDS–PAGE at 100–150 V for 1 h. The proteins were then transferred from the gel to PVDF membrane at 25 V. The blots were blocked with 3% BSA in TBST for 1 h at room temperature. The blots were incubated separately overnight at 4 °C with the following primary antibodies:

P-JNK monoclonal antibody (G-7: sc-6254, Santa Cruz Biotechnology, Inc, Oregon, USA), β-catenin polyclonal antibody (H-102: sc-7199, Santa Cruz Biotechnology, Inc, Oregon, USA), P-GSK-3β polyclonal antibody (Ser 9: sc-11757, Santa Cruz Biotechnology, Inc, Oregon, USA) (dilution 1 : 500). The membranes were washed thoroughly and incubated with the secondary conjugated antibody poly HRP anti-rabbit IgG (31460, Thermo Fisher Scientific, USA) (dilution 1 : 200) for 1 h at room temp. The membranes were re-washed and the signal was detected by a chemiluminescent substrate, Thermo Fisher Scientific, USA. The images were captured using a CCD camera-based imager and the band intensity of each protein was determined using Image J analysis software (Bitplane, USA).

2.9. Microbiome determination and analysis

Fecal pellets were collected from each animal, the collected samples within the same group were, pooled and kept at −80 °C freezer until DNA extraction.[33,34] The DNA extraction was done using the homogenized pooled samples and using the GeneJet Genomic DNA purification Kit (Thermo Scientific, cat. no. K0721). The DNA concentration and quality were checked using PicoGreen, Qubit® fluorimeter.

2.9.1. Library preparation. 16S rDNA gene amplicons were obtained following the 16S rDNA gene Metagenomic Sequencing Library Preparation Illumina protocol (Cod. 15044223 Rev. A). The gene-specific sequences used in this protocol target the 16S rDNA gene V3 and V4 region. Illumina adapter overhang nucleotide sequences were added to the gene-specific sequences. The primers were selected from ref. 35. The full-length primer sequences are 16S rDNA gene amplicon PCR forward primer = 5′TCGTCGGCAGCGTCAGATGTGTATAAGAGACAGCCTACGGGNGGCWGCAG3′. 16S rDNA gene amplicon PCR reverse primer = 5′GTCTCGTGGGCTCGGAGATGTGTATAAGAGACAGGACTACHVGGGTATCTAATCC3′. The microbial genomic DNA (5 ng μL^{-1} in 10 mM Tris pH 8.5) was used to initiate the protocol. After 16S rDNA gene amplification, the multiplexing step was performed using the Nextera XT Index Kit (FC-131-1096). 1 μL of the PCR product was run on a Bioanalyzer DNA 1000 chip to verify the size, the expected size on a Bioanalyzer trace was ∼550 bp. After size verification, the libraries were sequenced using a 2 × 300 pb paired-end run (MiSeq Reagent kit v3 (MS-102-3001)) on a MiSeq Sequencer according to manufacturer's instructions (Illumina).

2.9.2. Quality assessment and sequence joining. Quality assessment was performed by the use of prinseq-lite program.[36]

Applying the following parameters: min_length: 50; trim_-qual_right: 30; trim_qual_type: mean; trim_qual_window: 20; R1 and R2 from Illumina sequencing where joined using FLASH program.

2.9.3. Bioinformatic analysis. Data were obtained using an *ad hoc* pipeline written in R Statistics environment,[37] making use of several open source libraries such as *gdata* and *vegan*. The sequence data have been analyzed using QIIMM2 pipeline.[38] Metataxonomy analysis: metataxonomy analysis was performed using some of Qiime2 plugins. Denoising and chimera removing were performed starting from paired ends data using DADA2 pipeline.[39]

2.9.4. Taxonomic assignation. Taxonomic affiliations have been assigned using the Naive Bayesian classifier integrated into QIIMM2 plugins. The database used for this taxonomic assignation was the SILVA_release_132.[40] *KRONA* viewer report has been generated using Krona hierarchical browser.[41]

2.10. Statistical analysis

SPSS software version 22 (SPSS Inc., Chicago, Illinois) was used for the statistical analysis of the results. One way analysis of variance (ANOVA) followed by *post hoc* Tukey's test was used to examine for the statistical significance among groups. A p-value < 0.05 was considered to be statistically significant. Data were represented as mean $\pm$ SE.

3. Results

3.1. Effect of pre-, pro- and synbiotic treatments on the mice body weight

We followed the change in the mice body weight throughout the experimental period to evaluate the possible effects of our studied pre-, pro- and synbiotic treatments. The results showed a significant difference between the body weight of the control group and the DMH-treated group only at week 24 of the experiment at which DMH administration significantly decreased the mice body weight ($p < 0.01$). Interestingly, administration of prebiotic decreased the body weight significantly at weeks 8, 12, 16, 20 and 24 compared to the control group ($p < 0.01$) and at weeks 20 and 24 compared to the DMH group at $p < 0.01$. In addition, administration of probiotic decreased the body weight significantly at weeks 8,12,16, 20 and 24 compared to the control group ($p < 0.01$) and at weeks 12, 16, 20 and 24 compared to DMH group ($p < 0.01$). Similarly, the mice body weights of the synbiotic were decreased significantly at weeks 8, 12, 16, 20 and 24 compared to the control group and at weeks 20 and 24 compared to the DMH group ($p < 0.01$). These results indicate that administration of the prebiotic, probiotic or both treatments has a prominent body weight reducing effect (Fig. 1).

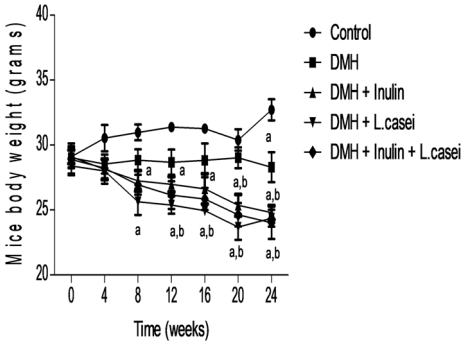

Fig. 1 Effect of the treatments on mice body weight. Line chart shows the mice body weights of the control, DMH, DMH + inulin, DMH + *L. casei* and DMH + inulin + *L. casei*, evaluated at 4 weeks interval till the sacrifice day. [a]Significantly different from control group ($p < 0.01$). [b]Significantly different from DMH group ($p < 0.01$).

3.2. Effect of pre-, pro- and synbiotic treatments on the biochemical measurements

To explain the mechanism by which our treatments reduced the animals' body weights, we measured the blood glucose, triglycerides and total cholesterol levels at the end of the experiment. The results showed no significant difference in the blood glucose, total cholesterol or triglycerides concentrations between the DMH-treated and the control groups. However, the blood glucose and total cholesterol levels were significantly reduced in the prebiotic, probiotic and synbiotic treated groups compared to the control or DMH-treated groups at $p < 0.05$. In addition, the blood triglycerides level was reduced significantly in the symbiotic-treated group compared to both the control and DMH-treated groups at $p < 0.05$ (Table 1). These results indicate the potential hypoglycemic and the lipid-lowering effect of our treatments that ultimately lead to a reduction in body weight.

3.3. Effect of pre-, pro- and synbiotic treatments on the colon macroscopic and microscopic architecture

The macroscopic examination of the entire colon showed a formation of multi-plaque lesions in the DMH-treated group compared to the control group. However, there was an apparent decrease in the number of plaque lesions in the prebiotic treated group and probiotic treated group with a complete absence of plaque lesions in the synbiotic-treated group (Fig. 2).

Further examination of the colon tissues at the microscopic scale using H&E staining showed that 75% of the examined samples of DMH-treated group exhibited signs of both inflammation and adenoma development compared to the control group. Moreover, 100% of the examined samples of DMH-treated group exhibited severe loss of goblet cells, aberrant colonic crypt, hyperplasia, and dysplasia compared to the control group. 62.5% of the DMH group showed adenocarcinoma. Remarkably, the prebiotic treated group showed a decrease in the degree of inflammation and loss of the goblet cells to 40%, in addition, the formation of aberrant colonic crypts decreased to 60% with no signs of dysplasia, hyperplasia or adenocarcinoma. Similar observations were recorded in the case of probiotic-treated group where the signs of inflammation and loss of goblet cells decreased to 20%, the aberrant colonic crypts were reduced to 40% with no signs of dysplasia or adenocarcinoma. In the synbiotic treated group, the results

Table 1 Effect of the pre-, pro- and synbiotic treatments on blood glucose, total cholesterol and triglycerides levels

	Blood glucose (mg dl^{-1})	Total cholesterol (mg dl^{-1})	Triglycerides (mg dl^{-1})
Control	108.83 ± 22.80	103.22 ± 15.51	86.33 ± 18.57
DMH	85.01 ± 20.78	92.52 ± 14.98	87.42 ± 28.01
DMH + inulin	58.12 ± 23.67^{b}	66.44 ± 27.78^{a}	53.87 ± 16.06
DMH + *L. casei*	58.66 ± 34.04^{b}	60.88 ± 24.18^{a,c}	72.12 ± 35.23
DMH + inulin + *L. casei*	53.71 ± 21.19^{b}	56.28 ± 21.95^{b,c}	46.42 ± 10.58^{a,c}

^{a} Significantly different from the control group ($p < 0.05$). ^{b} Significantly different from the control group ($p < 0.01$). ^{c} Significantly different from the DMH group ($p < 0.05$).

showed no signs of inflammation, aberrant colonic crypt, loss of the goblet cells, dysplasia or adenocarcinoma (Fig. 3A–C).

Interestingly, estimating the number of ACF in each colon/group by methylene blue staining revealed that, in the control group, there were normal crypts without ACF formation. Although the DMH treated group showed an increased number of ACF that reached 12.1 ± 0.56 ACF per focus. Importantly, administration of probiotic, prebiotic and synbiotic significantly decreased the number of ACF by three, five and six times respectively compared to the DMH-treated group ($p < 0.001$) (Fig. 4A and B). Additionally, the percentages of goblet cells in pre-, pro- and synbiotic groups were estimated as 61.7%, 81.7% and 97.7% respectively compared with the DMH group that showed 0% of goblet cells (Fig. 4C).

3.4. Effect of pre-, pro- and synbiotic treatments on CEA expression

To confirm the histopathology findings, we immuno-stained the colon tissues with CEA antibody. Our results showed an increased expression of CEA in the DMH-treated group by 37 folds compared to the control group ($p < 0.001$). However, the prebiotic, the probiotic and synbiotic groups showed a significant reduction in the CEA expression estimated by six, three and 19 folds respectively, compared to the DMH-treated group at $p < 0.001$ (Fig. 5A and B).

3.5. Effect of pre-, pro- and synbiotic treatments on the expression of p-JNK-1, p-GSK3-β and β-catenin proteins

To identify the molecular pathway targeted by our treatments that may explain their protective effects against colon carcinogenesis, we measured the protein expression level of β-catenin, the master gene in regulating the colon cancer development, with its regulatory proteins; p-JNK-1, and p-GSK3β. The findings demonstrated that DMH-treated group showed a significant decrease in the expression of p-JNK-1 by two and a half folds but an increase in the expression of β-catenin and p-GSK3β proteins by seven and five folds, respectively compared to the control group at $p < 0.05$ (Fig. 6). Interestingly, administration of prebiotic resulted in a significant increase in the expression level of p-JNK-1 protein by six folds while decreasing the

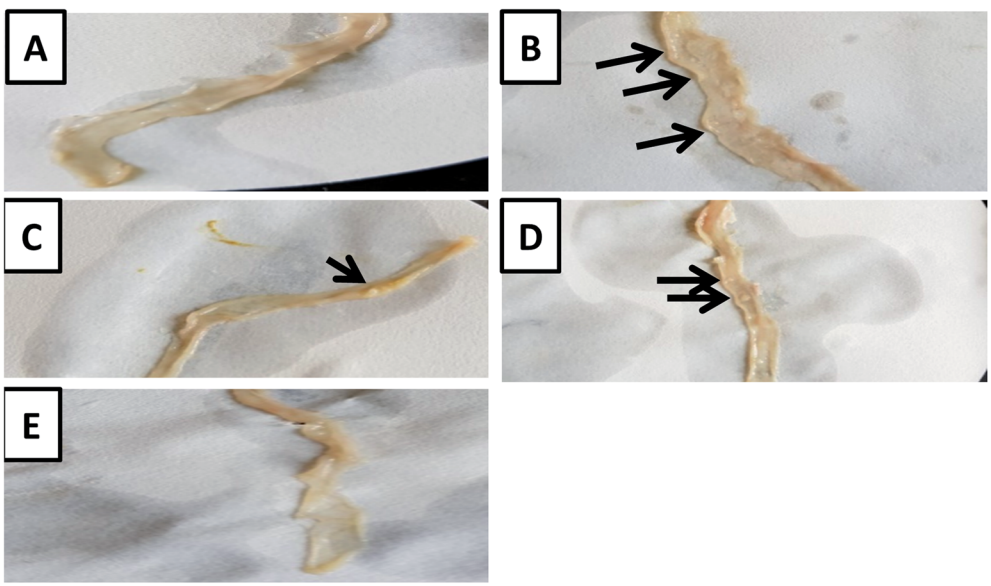

Fig. 2 Macroscopic examination of the colons. (A) A photo-macrograph of the entire colon from normal control group showing no plaque lesions. (B) A photo-macrograph of the entire colon from the DMH-treated group showing multiple plaque lesions. (C) A photo-macrograph from the DMH + inulin treated group showing one plaque lesion. (D) A photo-macrograph from the DMH + *L. casei* treated group showing two plaque lesions. (E) A photo-macrograph from the DMH + inulin + *L. casei* treated with no plaque lesions that can be seen.

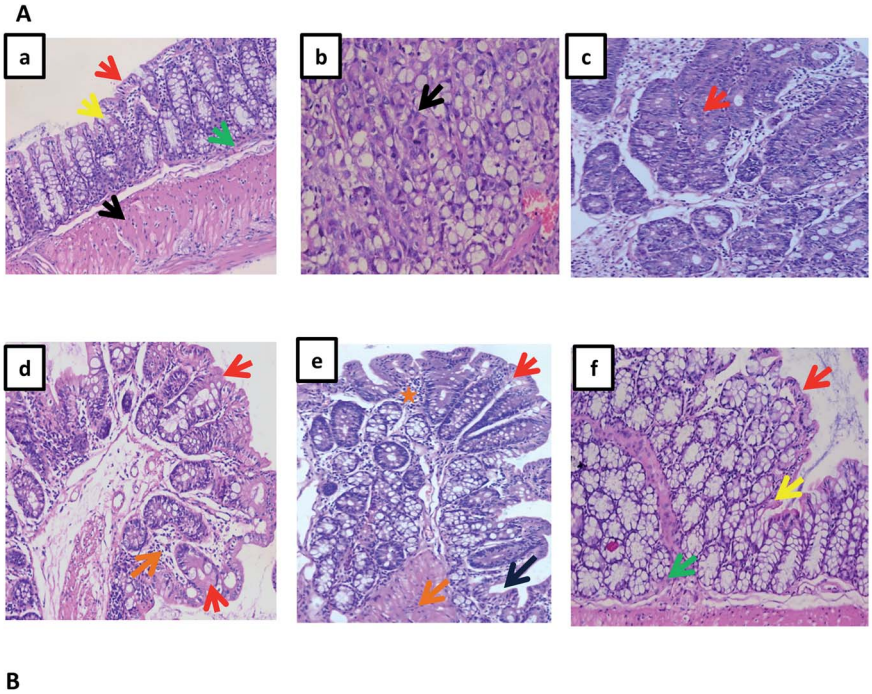

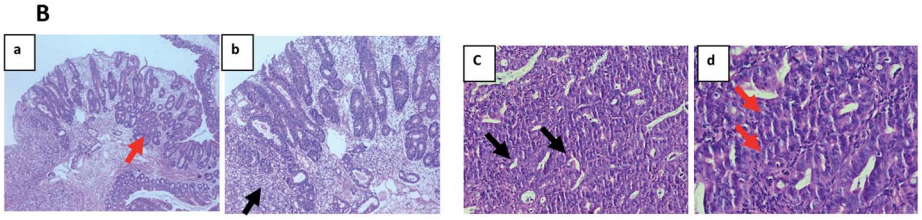

C

	Inflammation	Aberrant colonic crypt	Loss of goblet cells	Hyperplasia/ dysplasia	Adenoma Mean+ SE (Incidence)	Adenocarcinoma Mean+ SE (Incidence)
Control	Nil	Nil	Nil	Nil	0 ± 0 (0/8)	0 ± 0 (0/8)
DMH- group	75%	100%	100%	100%	2.12 ± 0.48 **a** (6/8)	0.62 ± 0.18 **a** (5/8)
DMH+ inulin	40%	60%	40%	Nil	0.87 ± 0.35 (4/8)	0 ± 0 **b** (0/8)
DMH+ L.casei	20%	40%	20%	Nil	0.62 ± 0.32 **b** (5/8)	0 ± 0 **b** (0/8)
DMH+ inulin+ L.casei	Nil	Nil	Nil	Nil	0.50 ± 0.26 **b** (3/8)	0 ± 0 **b** (0/8)

Fig. 3 Microscopic examination of the colon tissues. (A) H&E staining of the colon sections. (a) Colon tissue from the control group showing normal mucosa lined with columnar mucin-secreting cells (red arrow) overlying crypts (yellow arrow) with normal muscularis mucosa (green arrow) and normal muscle tissue (black arrow). (b and c) Colon tissues from the DMH-treated group. (b) Colonic mucosa showing malignant colonic acini forming irregular tubular structures, with nuclear stratification, multiple lumens and reduced stroma ("back to back") invading lamina and muscle layer ((b) black arrow), (c) colonic mucosa showing crowded, back to back colonic glands lined with hyperplastic and dysplastic epithelial cells ((c) red arrow). (d) Colon tissues from the DMH + inulin treated group, showing colonic mucosa lined with columnar mucin-secreting cells with regenerative changes (red arrow) and chronic inflammatory cells (orange arrow). (e) Colon tissues from the DMH + *L. casei* treated group, showing colonic mucosa lined with columnar mucin-secreting cells (red arrow) with regenerative changes (dark blue arrow), chronic inflammatory cells (orange arrow) and inflammatory cells (orange star). (f) Colon tissues from the DMH + inulin + *L. casei* treated group, showing almost normal mucosa lined with columnar mucin-secreting cells (red arrow) overlying crypts (yellow arrow) with normal muscularis mucosa (green arrow). 400×. (B) H&E staining of DMH-treated colon tissues showing adenoma and adenocarcinoma. (a and b) Colonic mucosa of DMH group showing both tubular adenoma with high grade dysplasia and malignant changes. (a) Colonic mucosa showing crowded, back to back colonic glands lined with hyperplastic and dysplastic epithelial cells (red arrow), 100×. (b) Colonic mucosa showing malignant colonic acini, malignant irregular sheets of mucin secreting cells with signet cell differentiation, invading lamina and muscle layer (black arrow), 200×. (c) Colonic mucosa of DMH group showing malignant colonic acini, malignant acini forming irregular tubular structures, with nuclear stratification (black arrow), 100×. (d) Multiple lumens and reduced stroma ("back to back") (red arrow) invading lamina and muscle layer are seen, 400×. (C) Table shows the percentage of incidence of the histopathological changes in groups. [a]Significantly different from control group ($p < 0.001$). [b]Significantly different from DMH group ($p < 0.001$). Number of mice is 8 per group.

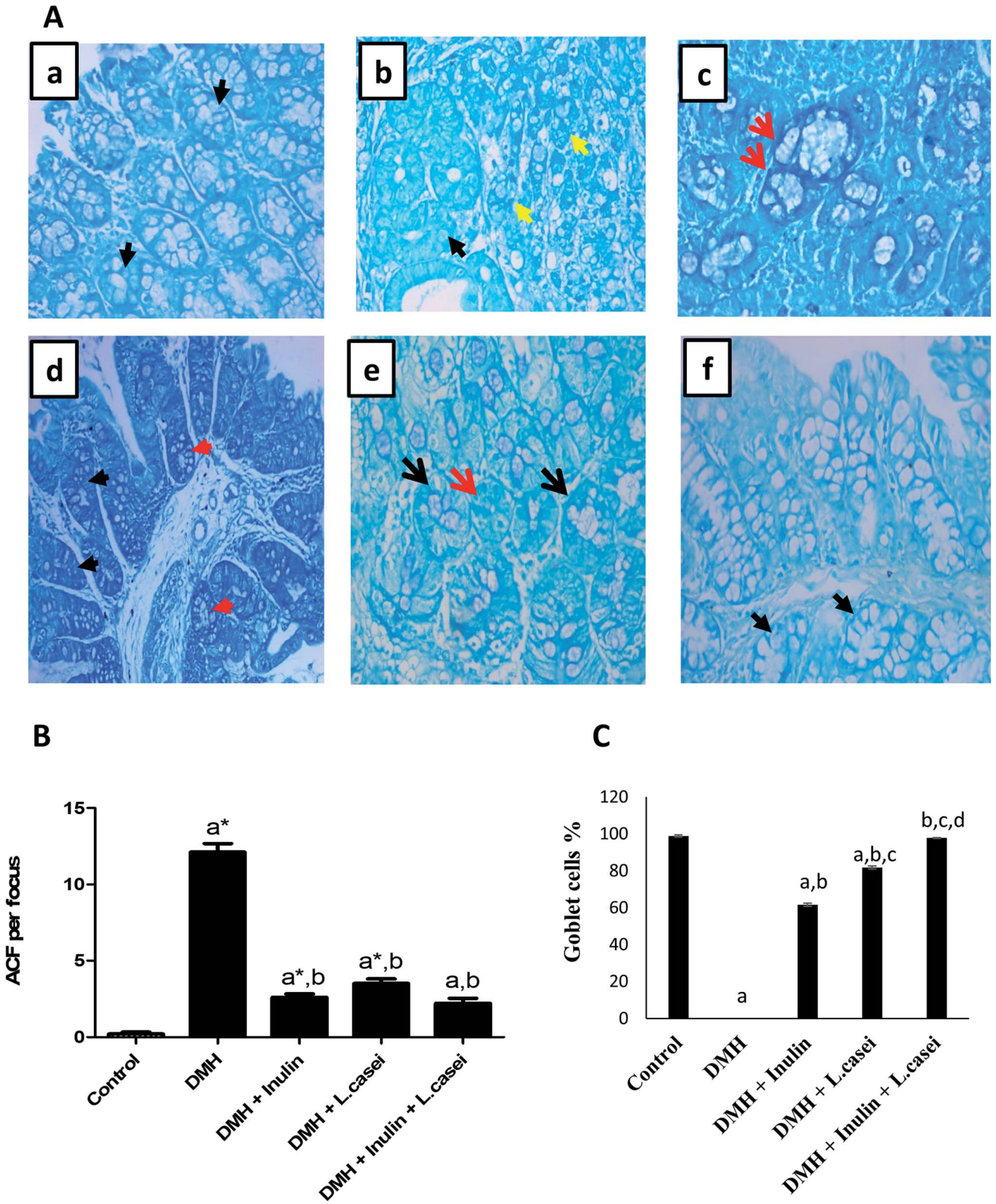

Fig. 4 Methylene blue staining of the aberrant crypt foci among the studied groups. (A) Photomicrograph of colon tissues showing aberrant crypt foci. (a) Colonic section from the control group stained with methylene blue showing normal crypts (black arrow). (b and c) Colonic sections from the DMH-treated group showing tumoral signet ring cells (yellow arrow) and normal crypts can be seen (black arrow). (d) Colonic section from the DMH + inulin treated group showing few aberrant colonic crypt foci (red arrow) and normal crypts (black arrow). (e) Colonic section from the DMH + *L. casei* treated group showing scattered aberrant colonic crypts (red arrow) and normal crypts (black arrow). (f) Colonic section from the (DMH + inulin + *L. casei*) treated group showing normal crypts (black arrow), ×400. (B) Quantification of the colonic ACF per focus in the studied groups, (C) Quantification of the goblet cells in the studied groups. Data are represented as mean ± SE. [a]Significantly different from control group ($p < 0.01$). [a*]Significantly different from control group ($p < 0.001$). [b]Significantly different from DMH group ($p < 0.001$). [c]Significantly different from DMH + inulin group ($p < 0.001$). [d]Significantly different from DMH + *L. casei* group ($p < 0.001$).

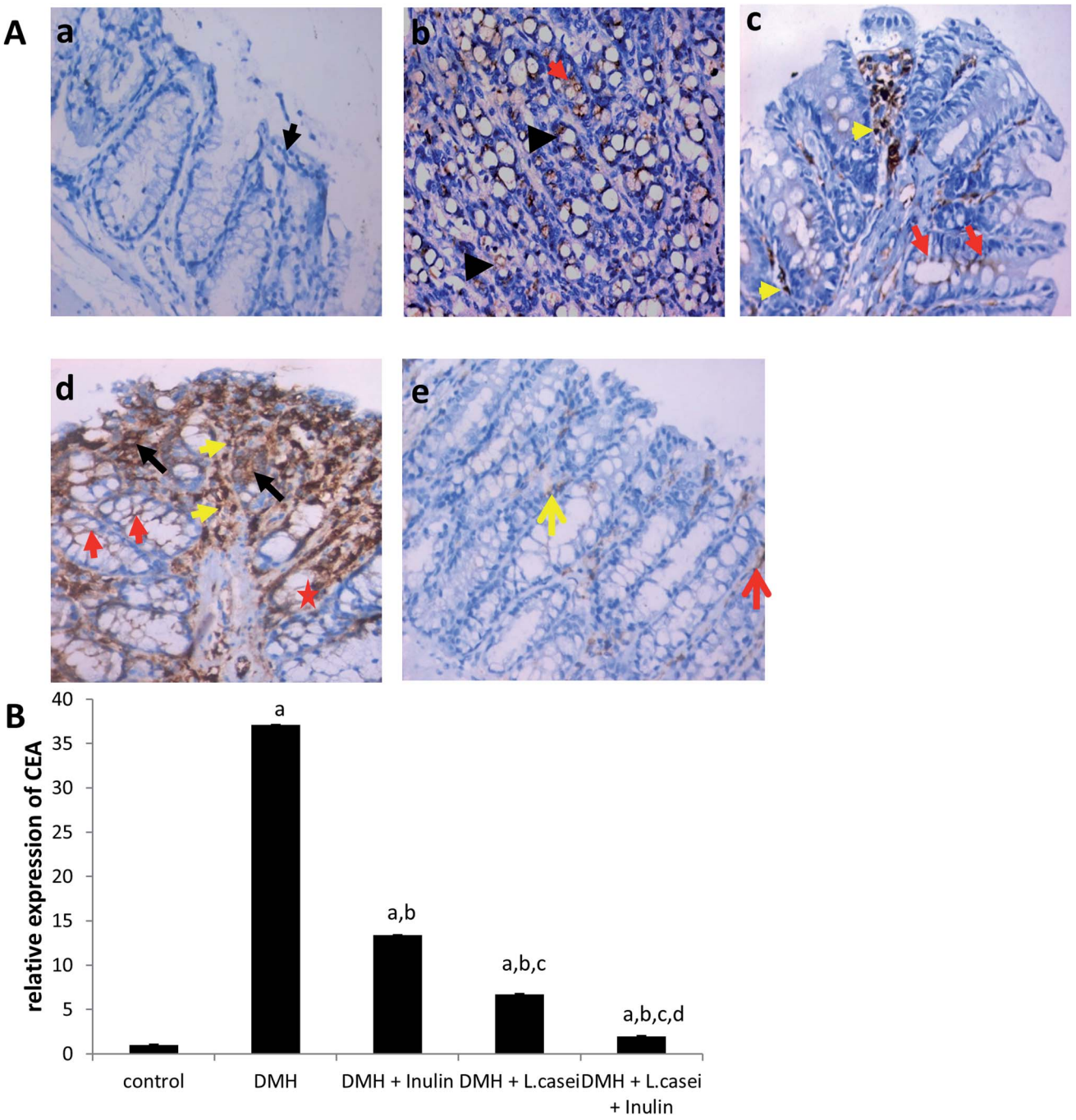

Fig. 5 The CEA expression in the colon tissues among the studied group. (A) Photomicrograph of mice colon tissues showing the expression level of CEA. (a) Colon tissue from the control group showing normal mucosa with negative CEA expression (black arrow). (b) Colonic mucosa from the DMH-treated group showing high expression level of CEA was no longer restricted to the apical surface (red arrow points to apical surface staining) and significant intracellular localization of CEA in the malignant cells (black arrows). (c) Colon tissues from the (DMH + inulin) group showing mild expression level of CEA in the apical surface (red arrow points to apical surface staining) and positive staining of inflammatory cells (yellow arrow). (d) Colon tissues from the (DMH + *L. casei*) treated group showing moderate expression of CEA in the apical surface of crypts (red arrow points to apical surface staining & red star point to basolateral staining) and significant intracellular localization of CEA in aberrant colonic crypts (black arrow) in addition to a positive staining of inflammatory cells (yellow arrow). (e) Colon tissues from the (DMH + inulin + *L. casei*) treated group showing minimal expression level of CEA restricted to the apical surface (red arrow points to apical surface staining), positive staining of inflammatory cells (yellow arrow), ×400. (B) Quantification of the expression level of CEA. Column figure shows the relative expression level of CEA on (*Y*-axis) among control, DMH, DMH + inulin, DMH + *L. casei* and DMH + inulin + *L. casei* treated groups on (*X*-axis). Number of mice is 8 per group. Data are represented as mean ± SE. [a]Significantly different from control group ($p < 0.001$). [b]Significantly different from DMH group ($p < 0.001$). [c]Significantly different from DMH + inulin group ($p < 0.001$). [d]Significantly different from DMH + *L. casei* group ($p < 0.001$).

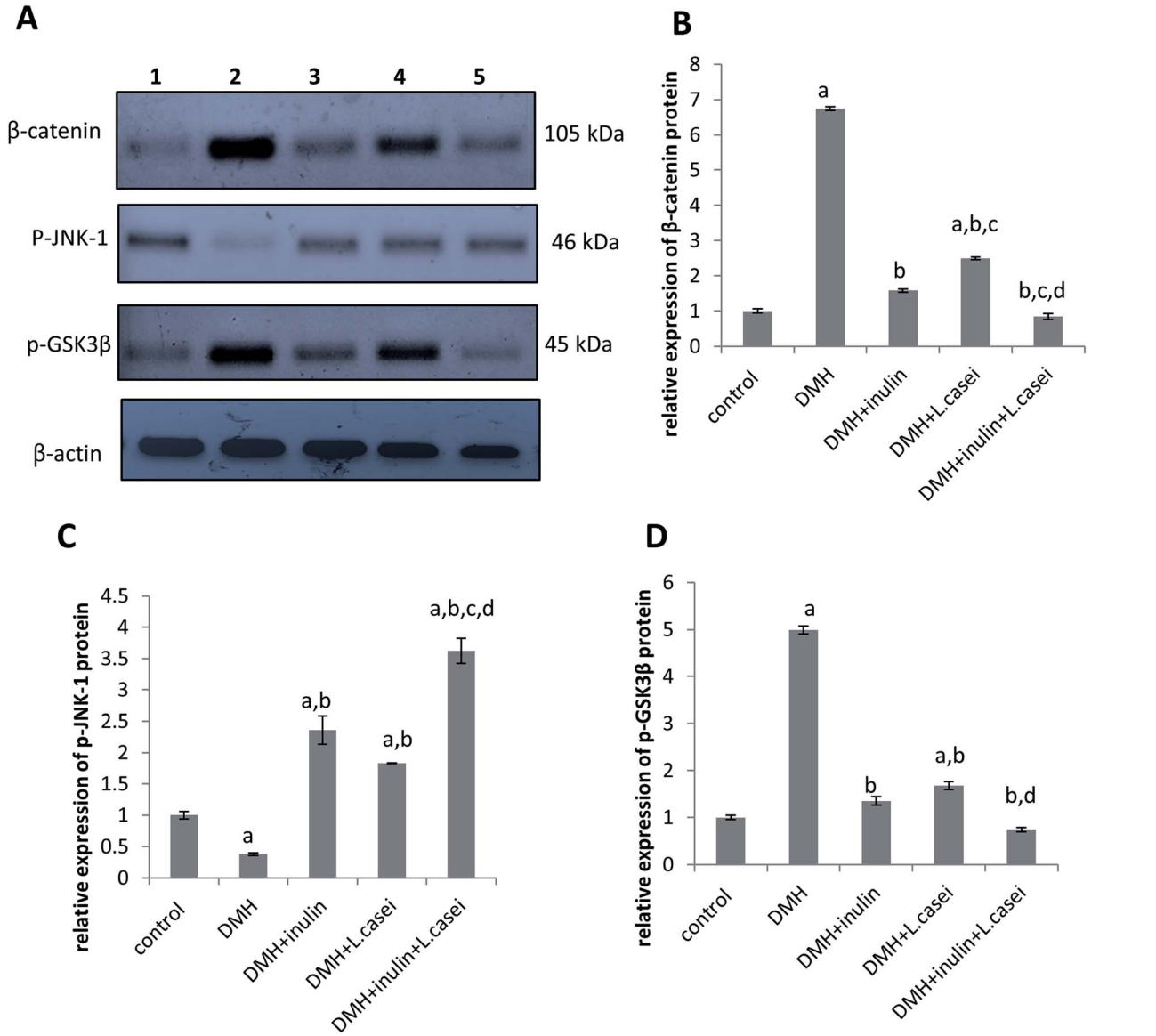

Fig. 6 Western blotting of β-catenin, p-JNK-1 and p-GSK3β expression in colonic tissues from the studied group. (A) Western blot analysis of β-catenin, p-JNK-1 and p-GSK3β proteins expression *versus* housekeeping protein β-actin in the following order: Lane 1: control group, Lane 2: DMH group, Lane 3: DMH + inulin group, Lane 4: DMH + *L. casei* group and Lane 5: DMH + inulin + *L. casei* group. (B) The quantitative densitometry of the expression level of β-catenin protein. (C) The quantitative densitometry of the expression level of p-JNK-1, (D) the quantitative densitometry of the expression level of p-GSK3β. Number of mice is 8. Data are represented as mean ± SE. [a]Significantly different from control group ($p < 0.05$). [b]Significantly different from DMH group ($p < 0.05$). [c]Significantly different from inulin group ($p < 0.05$). [d]Significantly different from *L. casei* group ($p < 0.05$).

expression level of both β-catenin and p-GSK3β by four folds compared to the DMH-treated group at $p < 0.05$. In the same way, administration of probiotic increased the expression level of p-JNK-1 protein by five folds while decreasing the expression of β-catenin and p-GSK3β by three folds compared to the DMH-treated group at $p < 0.05$. Interestingly, the synbiotic-treated group showed an increased p-JNK-1 expression level by nine folds with a decreased expression of β-catenin and p-GSK3β proteins by eight and seven folds respectively compared to the DMH-treated group at $p < 0.05$ (Fig. 6).

3.6. Microbiome analysis

High-throughput sequencing resulted in 585 554 reads, average 117 110 reads per sample, more detailed results are found in ESI Tables S1–S7.† The data filtration resulted in reduction in the reads count, the highest reads count recorded was 114 847 in DMH treated group, while the lowest reads count was 57 980 in the control group (Fig. 7A). The total reads obtained were classified into 23 phyla, 40 classes, 103 orders, 201 families and 464 genera. Alpha diversity of the groups was calculated including Chao1, ACE and Fisher indices (Fig. 7A). The Shannon and Chao1 indices were highest at the synbiotic-treated

A

	Reads count by sample			Alpha diversity – Genus level		
	Input	Filtered	Non-chimeric	Chao1	ACE±SE	Shannon
Control	73617	59262	57980	243	243±7.68	2.37
DMH	150362	119594	114847	200	200± 6.35	3.33
DMH + Inulin	121299	96494	95251	245	245± 7.73	1.95
DMH + *L. casei*	111737	88378	85662	187	187.22± 6.28	3.08
DMH + *L. casei* + Inulin	128539	100553	97899	276	276± 8	2.88

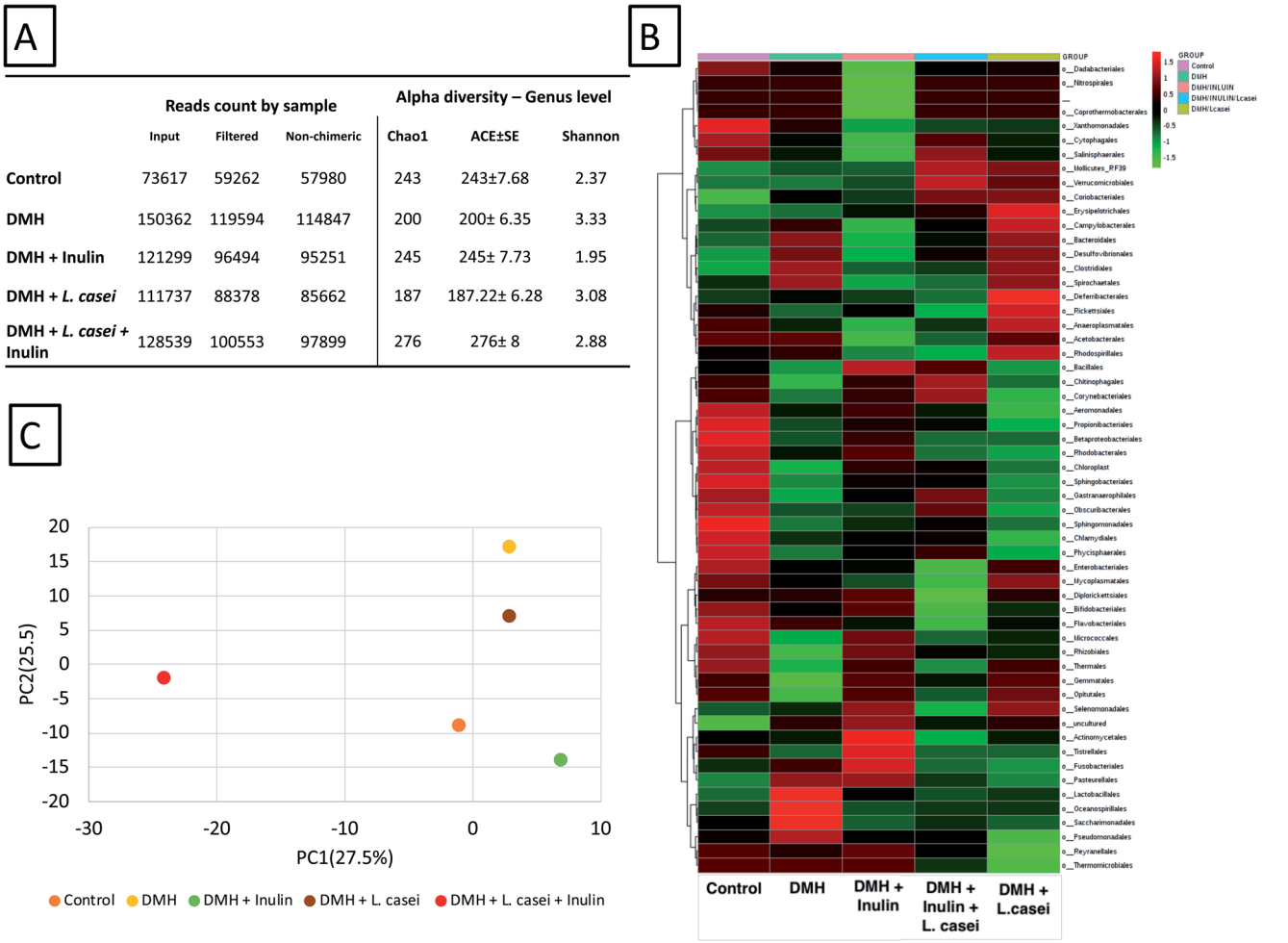

Fig. 7 Overview of the microbiome analysis. (A) The obtained reads count for the different groups used in the study showing the original and the filtered reads count. The alpha diversity factors Chao1, ACE and Shannon indexes are shown. (B) Heatmap representation of the microbiome results shown to the order level. (C) Principal component analysis PcoA determined based on the reads count per genus. The principal component 1 was calculated to 27.5% and PC2 was calculated to 25.5%. ClustVis webserver with a built-in program was used to calculate the principal components.

group. Fig. 7B shows the heatmap representation calculated at the order level of the classified reads obtained. Importantly, the principal component analysis among the five tested groups showed distinct separation of the synbiotic-treated group compared to all other sample groups (see also ESI Fig. S1†). The PC1 was computed at 27.5% while the PC2 was computed at 25.5% (Fig. 7C).

Fig. 8 shows the reads counts recorded for the highly represented bacterial phyla among the five tested groups. Interestingly the *Verrucomicrobia* phylum was enriched in animal groups treated with *L. casei* (probiotic group and synbiotic treated group). The major contribution to the phylum *Verrucomicrobia* is due to the genus *Akkermansia*, the only identified genus from this phylum. *Bacteroidetes* were found at highest abundance in the DMH treated group, while the lowest abundance was at the prebiotic treated group. On the contrary, *Firmicutes* were found at the lowest abundance at the DMH-treated group, while the highest abundance was found in the prebiotic treated groups.

The genus *Akkermansia* reads count were 1821 and 14 231 in the case of probiotic and synbiotic treated groups respectively compared to zero and 40 in the non-*L. casei* treated groups (DMH) and prebiotic respectively (Table 2). Similarly, the genus *Turicibacter* reads count were 1094 and 1841 in probiotic and synbiotic groups respectively compared to 681 and 465 reads count in the DMH and prebiotic treated groups respectively. Based on these observations, the genera *Akkermansia* and *Turicibacter* were significantly enriched in response to *L. casei* treatment (Table 2, $p < 0.05$).

4. Discussion

In the current study, we found that co-administration of *L. casei* and inulin as a synbiotic exhibited a superior protective effect against a DMH-induced colon cancer in male Swiss mice through affecting JNK-1/β-catenin signaling pathway as well as enriching beneficial bacteria in the colon such as *Akkermansia* and *Turicibacter*.

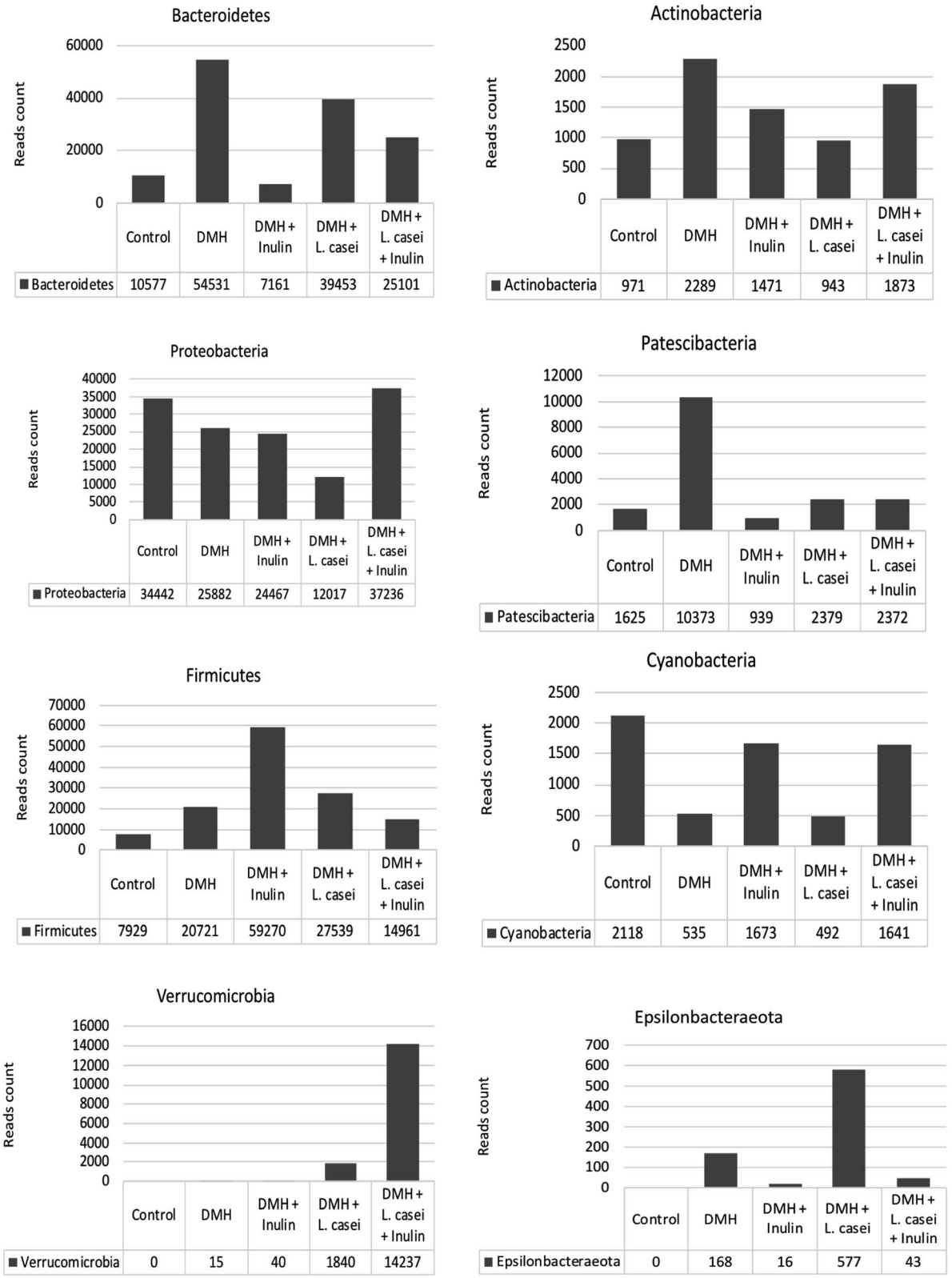

Fig. 8 Reads count for major phyla and genera. The reads count for the major phyla recorded among the different groups.

Our results showed no change in the body weight between the DMH-treated group and the control group except after 24 weeks of the experimental period which agrees with the previously published reports.[42] In addition, DMH showed no significant effect on calorie intake between groups.[43] However, in the current study, administration of inulin, *L. casei* or inulin +

Table 2 Bacterial genera significantly (Fisher's exact test) enriched in relation to *L. casei* or inulin administration in the treated groups

	Non-*L. casei*	*L. casei*	Total	*P* value
Genus *Akkermansia*				
DMH	0	1821	1821	0.0199
DMH + inulin	40	14 231	14 271	
Total	40	16 052	16 092	
Genus *Turicibacter*				
DMH	681	1094	1775	<0.00001
DMH + inulin	465	1841	2306	
Total	1146	2935	4081	
	Non-inulin	Inulin	Total	*P* value
Genus *Novosphingobium*				
DMH	8210	20 920	29 130	<0.00001
DMH + *L. casei*	9750	33 073	42 823	
Total	17 960	53 993	71 953	

L. casei together with DMH significantly decreased the body weight compared to either the control or the DMH groups. It is worthy to mention that the effect of administration of pre-, pro- or synbiotic formulations on the body weight in literature is controversial so far. For instance, it was observed that ingestion of inulin or fructo-oligosaccharides for long periods reduces the body weight.[44–47] Nevertheless, in other studies inulin administration had no effect or even increased the body weight of experimental animals.[48–50] On the same way, administration of different probiotics either showed a weight loss[51] or no effect on the body weight of mice.[52,53] Interestingly, it was found that administration of a synbiotic mixture (inulin plus *Lactobacillus acidophilus*, *Lactobacillus bulgaricus*, *Bifidobacterium bifidum*, *Bifidobacterium longum*, and *Streptococcus thermophilus*) for 5 weeks resulted in a decrease in the body weight of animals consistently with our findings.[54] Although, administration of *Bifidobacterium longum* BL999 with a prebiotic mixture (fructo-oligosaccharides and galacto-oligosaccharides) to infants from 14th to 112th day after birth resulted in a weight gain.[55]

In the current study, we did not record the food intake of animals throughout the experimental period. In literature, the administration of inulin in a model of DMH-induced colon cancer, showed no significant effect on food intake of animals although there was a significant reduction in the body weight compared to that of the normal rats.[56] On the same way, there was no significant difference in the food and water intake between mice given *Lactobacillus casei* and control mice although the *L. casei* group showed less blood glucose level and more protection from the diabetes incidence.[57,58] In an attempt to explain the body weight reducing effect, Drissi *et al.*, determined the differences in the genomes of some *Lactobacillus* species that have either weight protection or weight gain effect and they found that weight protecting *Lactobacillus* strains developed mechanisms for increased glycolysis and antioxidant defense.[59] In addition, *Lactobacillus* species decreased body weight through decreasing fatty acid synthase activity and hence white adipose tissue mass without any effect on energy intake.[60] These studies supporting our results that, the decrease in the blood glucose and lipids is partly responsible for the body weight reduction. Our results are also compatible with previous studies showing the reducing effect on inulin on blood glucose, total cholesterol and triglycerides levels in mice and humans.[50,61] On the same way, administration of *Lactobacillus casei* CCFM419 to mice with type 2 diabetes mellitus decreased the blood glucose level.[53] Interestingly, administration of a synbiotic formula to women suffering from polycystic ovary syndrome for 12 weeks resulted in decreased levels of plasma glucose, triglyceride, and cholesterol levels.[62]

Importantly, it was previously found that certain *Lactobacillus* strains isolated from human breast milk could combat cervical cancer *via* inducing apoptosis and inhibiting proliferation.[63] In particular, *L. casei* potentiated the antiproliferative effect of geniposide through the production of β-glucosidase in oral squamous cell carcinoma.[64] Remarkably, the anti-cancer activity of inulin was previously elucidated against melanoma as well as the transplanted mammary tumors in rats.[65] Moreover, inulin was found to decrease the preneoplastic lesions and multiplicity in colon cancer.[19] It acts through enhancing the healthy microflora which prevents the pathogenic bacteria from producing toxins or carcinogenic substances.[66] Our results support the previous studies and provide evidence that co-administration of *L. casei* and inulin exhibits a superior protective effect against colon cancer compared to the administration of either *L. casei* or inulin alone. This observation was seen in a significant decrease in CEA levels, ACF number as well as colon cancer morphological and histological changes in the synbiotic treated group compared to either pre- or probiotic treated groups.

There are several types of JNK proteins such as JNK-1, JNK-2, and JNK-3 involved in the regulation of various biological processes.[67,68] Although JNK-3 is only expressed in the brain and testis, both JNK-1 and JNK-2 proteins are ubiquitously expressed. JNK-1 was found to suppress the development of colon cancer through inhibiting the proliferation of intestinal epithelial cells and inducing apoptosis.[68–70] β-Catenin is a multifunctional overexpressed molecule in colorectal cancers.[71] Mutations in either β-catenin or adenomatous polyposis coli (APC) genes are commonly associated with the development of various cancer types especially, colon cancer.[72] Interestingly, β-catenin is regulated through its phosphorylation by GSK3β whereas, after its phosphorylation, a degradation complex is formed followed by ubiquitination and destruction by the proteasome.[73] Phosphorylation of GSK3β on Ser-9 leads to its inactivation which in turn prevents β-catenin degradation. Interestingly, JNK-1 activation decreases the phosphorylation of GSK3β.[73] Fang *et al.* 2010 described a reverse correlation between JNK-1 and β-catenin since JNK-1 decreases the activity of β-catenin.[20] Our novel findings indicate that administration of *L. casei*, inulin or both exhibit protective effects against DMH-induced colon cancer through increasing the expression of phosphorylated JNK-1 while decreasing the expression of phosphorylated GSK3β and ultimately β-catenin expression.

The bacterial flora of the gut is found in a dynamic balance with the host, and their composition is considered an indicator for the health status. It is worth mentioning that previous studies aimed to characterize the gut microbiome dysbiosis in relation to colon cancer showed conflicting results and no specific bacterial populations have been consistently linked to colon cancer.[74,75] We aimed in our microbiome analysis to trace the alteration in the bacterial taxa in response to different treatments. The results obtained revealed significant bacterial enrichment of the genera *Akkermansia* and *Turicibacter* to the animal groups treated with *L. casei* compared to those not treated with *L. casei*. Similarly, administration of inulin has resulted in significant enrichment of the genus *Novosphingobium* compared to animal groups not treated with inulin. *Akkermansia muciniphila* is anaerobic bacteria that was recently identified in the intestinal flora as a specialized mucin degrader.[76] Everard *et al.*, 2013 reported on the beneficial effect of *Akkermansia muciniphila* as a probiotic in which impairment of the mucin production by intestinal cells was related to colon cancer and can rational the reduction of *Akkermansia* in our DMH-treated group.[77] Derrien *et al.*, 2011 reported on the immune modulating effect of *Akkermansia muciniphila* in mice.[76] In addition, our results agree with the data obtained by Irecta-Nájera *et al.*, 2017, as they showed in their study the protective effect of *L. casei* on DMH-treated mice.[78] Previous studies reported on the beneficial effect of *Turicibacter* enrichment in the gut. *Turicibacter* has been correlated to the production of butyric acid, a short chain fatty acid, that act as an immunomodulators.[79] Moreover, an anti-inflammatory activity of *Turicibacter* bacteria has been suggested.[80,81] In the light of 95% similarity of the microbiome functional properties of the mouse and the human, based on Kyoto Encyclopedia of Genes and Genomes (KEGG) orthologous groups, the beneficial effect of the synbiotic treatment should be applicable to humans.[82]

5. Conclusion

Our novel findings indicate that administration of *L. casei*, inulin or their combination effectively protect from the development of colon cancer in male Swiss mice through targeting the JNK-1/β-catenin axis with the synbiotic treatment showing a superior effect. In addition, enhancing *Akkermansia* and *Turicibacter* beneficial bacteria in the colon was achieved. However, further studies are needed to elucidate if our pre-, pro- or synbiotic treatments have the same effect if used after the induction of colon cancer. In addition, it will be more informative to identify the main bacterial metabolites responsible for the protective effect against colon cancer.

Funding

This study did not receive a specific grant.

Conflicts of interest

Authors declare no conflict of interests.

Acknowledgements

Microbiome experiments and related data analysis were done by The Foundation for the Promotion of Health and Biomedical Research of Valencia Region, FISABIO, under supervision of Dr Giuseppe D'Auria, Valencia, Spain.

References

1 S. Roy and T. Chakraborty, Deciphering the molecular mechanism and apoptosis underlying the *in vitro* and *in vivo* chemotherapeutic efficacy of vanadium luteolin complex in colon cancer, *Cell Biochem. Funct.*, 2018, **36**, 116–128.
2 N. Sangeetha, S. Aranganathan and N. Nalini, Silibinin ameliorates oxidative stress induced aberrant crypt foci and lipid peroxidation in 1,2 dimethylhydrazine induced rat colon cancer, *Invest. New Drugs*, 2010, **28**, 225–233.
3 M. C. S. Mendes, *et al.*, Microbiota modification by probiotic supplementation reduces colitis associated colon cancer in mice, *World J. Gastroenterol.*, 2018, **24**, 1995.
4 C. Liu, *et al.*, Phytic acid improves intestinal mucosal barrier damage and reduces serum levels of proinflammatory cytokines in a 1,2-dimethylhydrazine-induced rat colorectal cancer model, *Br. J. Nutr.*, 2018, **120**, 121–130, DOI: 10.1017/s0007114518001290.
5 G. Y. Koh, *et al.*, *Parabacteroides distasonis* attenuates toll-like receptor 4 signaling and Akt activation and blocks colon tumor formation in high-fat diet-fed azoxymethane-treated mice, *Int. J. Cancer*, 2018, **143**, 1797–1805.
6 H. Svitina, *et al.*, Transplantation of placenta-derived multipotent cells in rats with dimethylhydrazine-induced colon cancer decreases survival rate, *Oncol. Lett.*, 2018, **15**, 5034–5042.
7 H. Svitina, *et al.*, Placenta-derived multipotent cells have no effect on the size and number of DMH-induced colon tumors in rats, *Exp. Ther. Med.*, 2017, **14**, 2135–2147.
8 E. Talero, *et al.*, Inhibition of chronic ulcerative colitis-associated adenocarcinoma development in mice by VSL# 3, *Inflamm. Bowel Dis.*, 2015, **21**, 1027–1037.
9 M.-T. Liong, Roles of probiotics and prebiotics in colon cancer prevention: postulated mechanisms and *in vivo* evidence, *Int. J. Mol. Sci.*, 2008, **9**, 854–863.
10 M. Kumar, *et al.*, Probiotic metabolites as epigenetic targets in the prevention of colon cancer, *Nutr. Rev.*, 2013, **71**, 23–34.
11 A. Tiptiri-Kourpeti, *et al.*, *Lactobacillus casei* exerts anti-proliferative effects accompanied by apoptotic cell death and up-regulation of TRAIL in colon carcinoma cells, *PLoS One*, 2016, **11**, e0147960.
12 M. L. Wan and H. El-Nezami, Targeting gut microbiota in hepatocellular carcinoma: probiotics as a novel therapy, *Hepatobiliary Surg. Nutr.*, 2018, **7**, 11.
13 R. A. B. Fagundes, T. F. Soder, K. C. Grokoski, F. Benetti and R. H. Mendes, Probiotics in the treatment of chronic kidney disease: a systematic review, *J. Bras. Nefrol.*, 2018, **40**, 278–286.

14 C.-C. Chen, *et al.*, Oral inoculation of probiotics Lactobacillus acidophilus NCFM suppresses tumour growth both in segmental orthotopic colon cancer and extra-intestinal tissue, *Br. J. Nutr.*, 2012, **107**, 1623–1634.

15 T. R. Qamar, *et al.*, Novel Combination of Prebiotics Galacto-Oligosaccharides and Inulin-Inhibited Aberrant Crypt Foci Formation and Biomarkers of Colon Cancer in Wistar Rats, *Nutrients*, 2016, **8**, 465.

16 A. Verma and G. Shukla, Administration of prebiotic inulin suppresses 1,2-dimethylhydrazine dihydrochloride induced procarcinogenic biomarkers fecal enzymes and preneoplastic lesions in early colon carcinogenesis in Sprague Dawley rats, *J. Funct. Foods*, 2013, **5**, 991–996.

17 A. Verma and G. Shukla, Synbiotic (*Lactobacillus rhamnosus* + *Lactobacillus acidophilus* + inulin) attenuates oxidative stress and colonic damage in 1,2-dimethylhydrazine dihydrochloride-induced colon carcinogenesis in Sprague–Dawley rats: a long-term study, *Eur. J. Cancer Prev.*, 2014, **23**, 550–559.

18 L. B. Bindels, *et al.*, Synbiotic approach restores intestinal homeostasis and prolongs survival in leukaemic mice with cachexia, *ISME J.*, 2016, **10**, 1456.

19 B. L. Pool-Zobel, Inulin-type fructans and reduction in colon cancer risk: review of experimental and human data, *Br. J. Nutr.*, 2005, **93**, S73–S90.

20 W. Fang, A. Han, X. Bi, B. Xiong and W. Yang, Tumor inhibition by sodium selenite is associated with activation of c-Jun NH2-terminal kinase 1 and suppression of β-catenin signaling, *Int. J. Cancer*, 2010, **127**, 32–42.

21 R. H. Giles, J. H. van Es and H. Clevers, Caught up in a Wnt storm: Wnt signaling in cancer, *Biochim. Biophys. Acta, Rev. Cancer*, 2003, **1653**, 1–24.

22 D. Hu, X. Bi, W. Fang, A. Han and W. Yang, GSK3β is involved in JNK2-mediated β-catenin inhibition, *PLoS One*, 2009, **4**, e6640.

23 J. Du, *et al.*, Anticancer activities of sulindac in prostate cancer cells associated with c-Jun NH2-terminal kinase 1/beta-catenin signaling, *Oncol. Lett.*, 2014, **8**, 313–316.

24 S. S. Piao and B. Shang, Pizotifen Inhibits the Proliferation and Migration of Colon Cancer HCT116 Cells by Down-regulating Wnt Signaling Pathway, *Ann. Clin. Lab. Sci.*, 2019, **49**, 183–188.

25 J.-H. Chang, Y. Y. Shim, S.-K. Cha, M. J. Reaney and K. M. Chee, Effect of Lactobacillus acidophilus KFRI342 on the development of chemically induced precancerous growths in the rat colon, *J. Med. Microbiol.*, 2012, **61**, 361–368.

26 J. D. Bancroft and M. Gamble, *Theory and practice of histological techniques*, Elsevier Health Sciences, 2008.

27 T. K. Motawi, S. A. El-Maraghy, A. N. ElMeshad, O. M. Nady and O. A. Hammam, Cromolyn chitosan nanoparticles as a novel protective approach for colorectal cancer, *Chem.-Biol. Interact.*, 2017, **275**, 1–12.

28 B. Shpitz, *et al.*, Proliferating cell nuclear antigen as a marker of cell kinetics in aberrant crypt foci, hyperplastic polyps, adenomas, and adenocarcinomas of the human colon, *Am. J. Surg.*, 1997, **174**, 425–430.

29 L. O. Whiteley, L. Hudson Jr and T. P. Pretlow, Aberrant crypt foci in the colonic mucosa of rats treated with a genotoxic and nongenotoxic colon carcinogen, *Toxicol. Pathol.*, 1996, **24**, 681–689.

30 Y. Jia, *et al.*, Metformin prevents DMH-induced colorectal cancer in diabetic rats by reversing the Warburg effect, *Toxicol. Pathol.*, 2015, **4**, 1730–1741.

31 S.-M. Hsu, L. Raine and H. Fanger, Use of avidin–biotin–peroxidase complex (ABC) in immunoperoxidase techniques: a comparison between ABC and unlabeled antibody (PAP) procedures, *J. Histochem. Cytochem.*, 1981, **29**, 577–580.

32 J. Waisberg, *et al.*, Padrão da distribuição tecidual do CEA no carcinoma colo-retal: relação com o nível sérico do CEA e classificação de Dukes, *Rev. Bras. Coloproctol.*, 2002, **22**, 7.

33 S. Yamada, *et al.*, Bile acid metabolism regulated by the gut microbiota promotes non-alcoholic steatohepatitis-associated hepatocellular carcinoma in mice, *Oncotarget*, 2018, **9**, 9925.

34 Y. Gendo, *et al.*, Dysbiosis of the Gut Microbiota on the Inflammatory Background due to Lack of Suppressor of Cytokine Signalling-1 in Mice, *Inflamm. Intest. Dis.*, 2018, **3**, 145–154.

35 A. Klindworth, *et al.*, Evaluation of general 16S ribosomal RNA gene PCR primers for classical and next-generation sequencing-based diversity studies, *Nucleic Acids Res.*, 2013, **41**, e1.

36 R. Schmieder and R. Edwards, Quality control and preprocessing of metagenomic datasets, *Bioinformatics*, 2011, **27**, 863–864.

37 R. C. Team, *A language and environment for statistical computing R Foundation for Statistical Computing*, Vienna, Austria, 2012, ISBN 3-900051-07-0.

38 J. G. Caporaso, *et al.*, QIIME allows analysis of high-throughput community sequencing data, *Nat. Methods*, 2010, **7**, 335.

39 B. J. Callahan, *et al.*, DADA2: high-resolution sample inference from Illumina amplicon data, *Nat. Methods*, 2016, **13**, 581.

40 C. Quast, *et al.*, The SILVA ribosomal RNA gene database project: improved data processing and web-based tools, *Nucleic Acids Res.*, 2012, **41**, D590–D596.

41 B. D. Ondov, N. H. Bergman and A. M. Phillippy, Interactive metagenomic visualization in a Web browser, *BMC Bioinf.*, 2011, **12**, 385.

42 V. Chithra and S. Leelamma, *Coriandrum sativum*—effect on lipid metabolism in 1, 2-dimethyl hydrazine induced colon cancer, *J. Ethnopharmacol.*, 2000, **71**, 457–463.

43 A. Lopez-Mejia, *et al.*, Chemopreventive effect of *Callistemon citrinus* (Curtis) Skeels against colon cancer induced by 1,2-dimethylhydrazine in rats, *J. Cancer Res. Clin. Oncol.*, 2019, **145**, 1417–1426.

44 C. Morris and G. A. Morris, The effect of inulin and fructo-oligosaccharide supplementation on the textural, rheological and sensory properties of bread and their role in weight management: A review, *Food Chem.*, 2012, **133**, 237–248.

45 N. M. Delzenne and P. D. Cani, Nutritional modulation of gut microbiota in the context of obesity and insulin resistance: Potential interest of prebiotics, *Int. Dairy J.*, 2010, **20**, 277–280.
46 P. D. Cani, *et al.*, Gut microbiota fermentation of prebiotics increases satietogenic and incretin gut peptide production with consequences for appetite sensation and glucose response after a meal, *Am. J. Clin. Nutr.*, 2009, **90**, 1236–1243.
47 K. R. Pandey, S. R. Naik and B. V. Vakil, Probiotics, prebiotics and synbiotics-a review, *J. Food Sci. Technol.*, 2015, **52**, 7577–7587.
48 S. Tan and J. A. Caparros-Martin, Isoquercetin and inulin synergistically modulate the gut microbiome to prevent development of the metabolic syndrome in mice fed a high fat diet, *Sci. Rep.*, 2018, **8**, 10100.
49 C. Andrieux, S. Lory, C. Dufour-Lescoat, R. De Baynast and O. Szylit, Physiological effects of inulin in germ-free rats and in heteroxenic rats inoculated with a human flora, *Food Hydrocolloids*, 1991, **5**, 49–56.
50 Q. Zhang, *et al.*, Inulin-type fructan improves diabetic phenotype and gut microbiota profiles in rats, *PeerJ*, 2018, **6**, e4446.
51 M. Million, *et al.*, Comparative meta-analysis of the effect of Lactobacillus species on weight gain in humans and animals, *Microb. Pathog.*, 2012, **53**, 100–108.
52 S. Yun, H. Park and J. Kang, Effect of *Lactobacillus gasseri* BNR17 on blood glucose levels and body weight in a mouse model of type 2 diabetes, *J. Appl. Microbiol.*, 2009, **107**, 1681–1686.
53 X. Li, *et al.*, Effects of *Lactobacillus casei* CCFM419 on insulin resistance and gut microbiota in type 2 diabetic mice, *Benefic. Microbes*, 2017, **8**, 421–432.
54 S.-C. Yang, *et al.*, Effect of synbiotics on intestinal microflora and digestive enzyme activities in rats, *World J. Gastroenterol.*, 2005, **11**, 7413.
55 G. Puccio, *et al.*, Clinical evaluation of a new starter formula for infants containing live *Bifidobacterium longum* BL999 and prebiotics, *Nutrition*, 2007, **23**, 1–8.
56 T. Qamar, *et al.*, Novel combination of prebiotics galacto-oligosaccharides and inulin-inhibited aberrant crypt foci formation and biomarkers of colon cancer in wistar rats, *Nutrients*, 2016, **8**, 465.
57 T. Matsuzaki, *et al.*, Effect of oral administration of *Lactobacillus casei* on alloxan-induced diabetes in mice, *APMIS*, 1997, **105**, 637–642.
58 H. Yadav, S. Jain and P. Sinha, Antidiabetic effect of probiotic dahi containing *Lactobacillus acidophilus* and *Lactobacillus casei* in high fructose fed rats, *Nutrition*, 2007, **23**, 62–68.
59 F. Drissi, *et al.*, Comparative genomics analysis of Lactobacillus species associated with weight gain or weight protection, *Nutr. Diabetes*, 2014, **4**, e109.
60 T. Arora, S. Singh and R. K. Sharma, Probiotics: interaction with gut microbiome and antiobesity potential, *Nutrition*, 2013, **29**, 591–596.
61 C. M. Williams, Effects of inulin on lipid parameters in humans, *J. Nutr.*, 1999, **129**, 1471S–1473S.
62 M. Samimi, A. Dadkhah and H. Haddad Kashani, The Effects of Synbiotic Supplementation on Metabolic Status in Women With Polycystic Ovary Syndrome: a Randomized Double-Blind Clinical Trial, *Probiotics Antimicrob. Proteins*, 2018, **10**, 1–7.
63 M. S. R. Rajoka, *et al.*, Anticancer potential against cervix cancer (HeLa) cell line of probiotic *Lactobacillus casei* and *Lactobacillus paracasei* strains isolated from human breast milk, *Food Funct.*, 2018, **9**, 2705–2715.
64 Y. Qian, *et al.*, *Lactobacillus casei* Strain Shirota Enhances the *In Vitro* Antiproliferative Effect of Geniposide in Human Oral Squamous Carcinoma HSC-3 Cells, *Molecules*, 2018, **23**, 1069.
65 H. S. Taper and M. Roberfroid, Influence of inulin and oligofructose on breast cancer and tumor growth, *J. Nutr.*, 1999, **129**, 1488S–1491S.
66 K. Kalyani Nair, S. Kharb and D. Thompkinson, Inulin dietary fiber with functional and health attributes—a review, *Food Rev. Int.*, 2010, **26**, 189–203.
67 A. Saadeddin, R. Babaei-Jadidi, B. Spencer-Dene and A. S. Nateri, The links between transcription, β-catenin/JNK signaling, and carcinogenesis, *Mol. Cancer Res.*, 2009, **7**, 1189–1196.
68 L. Hui, K. Zatloukal, H. Scheuch, E. Stepniak and E. F. Wagner, Proliferation of human HCC cells and chemically induced mouse liver cancers requires JNK1-dependent p21 downregulation, *J. Clin. Invest.*, 2008, **118**, 3943–3953.
69 C. Tong, *et al.*, c-Jun NH2-terminal kinase 1 plays a critical role in intestinal homeostasis and tumor suppression, *Am. J. Pathol.*, 2007, **171**, 297–303.
70 Q.-B. She, N. Chen, A. M. Bode, R. A. Flavell and Z. Dong, Deficiency of c-Jun-NH2-terminal kinase-1 in mice enhances skin tumor development by 12-*O*-tetradecanoylphorbol-13-acetate, *Cancer Res.*, 2002, **62**, 1343–1348.
71 T. Brabletz, *et al.*, Variable β-catenin expression in colorectal cancers indicates tumor progression driven by the tumor environment, *Proc. Natl. Acad. Sci. U. S. A.*, 2001, **98**, 10356–10361.
72 B. Javan, F. Atyabi and M. Shahbazi, Hypoxia-inducible bidirectional shRNA expression vector delivery using PEI/chitosan-TBA copolymers for colorectal Cancer gene therapy, *Life Sci.*, 2018, **202**, 140–151.
73 D. Hu, *et al.*, c-Jun N-terminal kinase 1 interacts with and negatively regulates Wnt/β-catenin signaling through GSK3β pathway, *Carcinogenesis*, 2008, **29**, 2317–2324.
74 H.-M. Chen, *et al.*, Decreased dietary fiber intake and structural alteration of gut microbiota in patients with advanced colorectal adenoma, *Am. J. Clin. Nutr.*, 2013, **97**, 1044–1052.
75 T. Wang, *et al.*, Structural segregation of gut microbiota between colorectal cancer patients and healthy volunteers, *ISME J.*, 2012, **6**, 320–329.
76 M. Derrien, M. C. Collado, K. Ben-Amor, S. Salminen and W. M. de Vos, The Mucin degrader *Akkermansia muciniphila* is an abundant resident of the human

intestinal tract, *Appl. Environ. Microbiol.*, 2008, **74**, 1646–1648.

77 A. Everard, *et al.*, Cross-talk between *Akkermansia muciniphila* and intestinal epithelium controls diet-induced obesity, *Proc. Natl. Acad. Sci. U. S. A.*, 2013, **110**, 9066–9071.

78 C. A. Irecta-Nájera, M. del Rosario Huizar-López, J. Casas-Solís, P. Castro-Félix and A. Santerre, Protective effect of *Lactobacillus casei* on DMH-induced colon carcinogenesis in mice, *Probiotics Antimicrob. Proteins*, 2017, **9**, 163–171.

79 Y. Zhong, M. Nyman and F. Fåk, Modulation of gut microbiota in rats fed high-fat diets by processing whole-grain barley to barley malt, *Mol. Nutr. Food Res.*, 2015, **59**, 2066–2076.

80 J. S. Suchodolski, Fecal Microbiome in Dogs with Acute Diarrhea and Idiopathic Inflammatory Bowel Disease, *Encyclopedia of Metagenomics: Environmental Metagenomics*, 2015, pp. 183–186.

81 T. Werner, *et al.*, Depletion of luminal iron alters the gut microbiota and prevents Crohn's disease-like ileitis, *Gut*, 2011, **60**, 325–333.

82 L. Xiao, *et al.*, A catalog of the mouse gut metagenome, *Nat. Biotechnol.*, 2015, **33**, 1103.